

Vibrationally resolved sum-frequency generation with broad-bandwidth infrared pulses

Lee J. Richter, Teresa P. Petralli-Mallow, and John C. Stephenson

National Institute of Standards and Technology, Gaithersburg, Maryland 20899

Received July 7, 1998

We present a novel procedure for vibrationally resolved sum-frequency generation (SFG) in which a broad-bandwidth IR pulse is mixed with a narrow-bandwidth visible pulse. The resultant SFG spectrum is dispersed with a spectrograph and detected in parallel with a scientific-grade CCD detector, permitting rapid and high signal-to-noise ratio data acquisition over a 400-cm^{-1} spectral region without scanning the IR frequency. Application to the study of a self-assembled monolayer of octadecanethiol is discussed.

OCIS codes: 190.0190, 190.4350, 240.0240, 240.6490, 320.7110, 240.0310.

Vibrationally resolved sum-frequency generation (SFG) spectroscopy, initially demonstrated by Shen and co-workers,¹ is a powerful probe of the molecular order at surfaces and interfaces.² In most SFG studies a narrow-bandwidth IR pulse mixes with a narrow-bandwidth visible pulse through a $\chi^{(2)}$ process at an interface to produce SFG that is not spectrally analyzed. The sum-frequency (SF) spectrum is laboriously acquired by means of scanning the wavelength of the IR pulse over the vibrational resonances. In this Letter we describe an alternative approach in which the SFG spectra are obtained with short acquisition times and without wavelength tuning. A nominally 100-fs laser system generates broad-bandwidth (BB) IR pulses that are mixed with narrow-bandwidth visible pulses at the interface of interest. The SF light is collected and dispersed in a spectrograph. A scientific-grade CCD detector is used to detect all the SF light (spectral range, 600 cm^{-1}) in parallel. The spectral resolution of this approach is determined by the spectrograph and the bandwidth of the nonresonant visible pulse. This BB SFG approach, using a tabletop commercial laser system, rapidly produces excellent spectra and, in principle, permits ultrafast time resolution.

Figure 1 details the optical system based on an optical parametric amplifier (OPA) pumped at a 1-kHz repetition rate by a Ti:sapphire regenerative amplifier^{3,4} that produces 800-nm pulses with 100-fs FWHM duration,⁵ 12-nm FWHM bandwidth, and $>800\text{-}\mu\text{J}$ energy. In the OPA a two-pass type II BBO crystal seeded by a white-light continuum produces signal and idler pulses with a combined energy of $>220\text{ }\mu\text{J}$. The OPA tunes with nearly constant combined power over the range of signal wavelengths from 1200 to 1600 nm. Autocorrelation of the signal at 1311 nm indicates pulses with 100 fs FWHM duration. The signal and the idler bandwidths are 43 nm at 1311 nm and 110 nm at 2091 nm, respectively. The pulse-to-pulse stability of the total OPA energy is 5%.⁶

BB tunable IR pulses are generated by difference-frequency (DF) mixing of the signal and the idler of the OPA in a 2-mm AgGaS_2 crystal that is $\lambda/4$ antireflection coated on input at $1.6\text{ }\mu\text{m}$ and on output

at $5.0\text{ }\mu\text{m}$. The scheme is comparable with that reported in Ref. 7. The orthogonally polarized signal and idler pulses are separated by a dichroic mirror (BS in Fig. 1), retimed for optimal overlap, and combined collinearly on a second dichroic mirror. The beams are unfocused, and a near-IR camera measures the spatial profile of the signal at the DF crystal to be $2.8\text{ mm} \times 3.4\text{ mm}$.⁸ The signal and the idler pulses are separated from the IR with a dichroic long-pass (LP) filter. A total of $180\text{ }\mu\text{J}$ combined signal and idler focused onto the DF crystal produces $6\text{-}\mu\text{J}$ pulses at $3.4\text{ }\mu\text{m}$, with a FWHM bandwidth of $0.3\text{ }\mu\text{m}$ (250 cm^{-1}) and a pulse duration of $\sim 0.22\text{ ps}$ FWHM (measured by autocorrelation). As the OPA and DF crystals are tuned, the IR pulse energy is $>3\text{ }\mu\text{J}$ from 3 to $8\text{ }\mu\text{m}$ (the long-wavelength cutoff of our IR spectrometer). The pulse-to-pulse stability of the IR energy is 9%.

We explored several ways to produce narrow-bandwidth visible pulses for the SFG. The most successful to date is diagrammed in Fig. 1. After two passes through the four-pass compressor, the amplified 800-nm pulses are spectrally dispersed and $\sim 100\text{ ps}$ long; the blue edge of the pulse is stripped

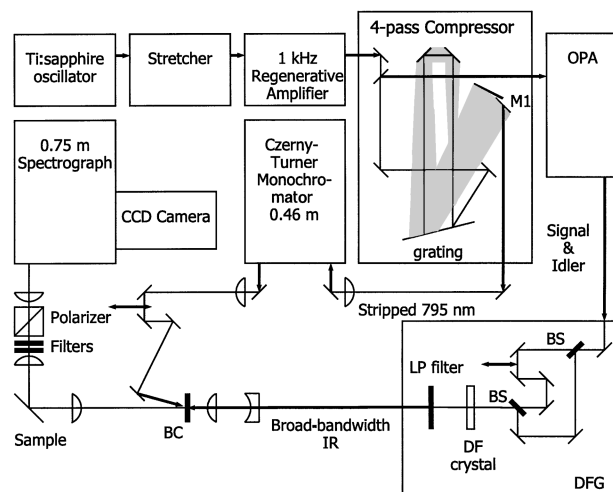


Fig. 1. Schematic diagram of the optical system. DFG, different-frequency generator. See text for other definitions.

from the beam with mirror M1. The removal of 80 μJ of amplified light produces a slight (linear) decrease in the OPA energy. This stripped beam is both spatially and temporally chirped. However, the area of the stripped beam is comparable with the spot size of the collimated beam that first strikes the grating, and the spatial chirp is pseudoscrambled. The bandwidth of the stripped beam is 50 cm^{-1} FWHM, and the measured frequency chirp is approximately $1.8\text{ cm}^{-1}/\text{ps}$. A homebuilt 46-cm focal-length (FL) symmetric Czerny–Turner monochromator with 1740-groove/mm provides a variable reduction in bandwidth and partially compensates for the remaining temporal chirp on the beam. The duration of the 795-nm output of the monochromator (75% energy efficient) is 7 ps FWHM for bandwidths from 2.5 to 20 cm^{-1} FWHM, and the pulse energy is nominally linear in bandwidth.

The visible and the IR pulses are polarization selected, brought to temporal and spatial overlap on a dichroic mirror (BC in Fig. 1), and focused with a simple 10-cm FL CaF_2 lens onto the sample at an incidence angle of 45° . As the lens is not an achromat, the IR focus is 4 mm beyond the 795-nm focus. In the SFG experiments we positioned the sample beyond the 795-nm focus to avoid sample damage by the visible beam. The areas of the visible and the IR spots at the sample were approximately 10^{-4} cm^2 and $4 \times 10^{-5}\text{ cm}^2$, respectively. Typical operating conditions, set by transport losses and inefficiency in the combining mirror, were 3 and 4 μJ for 3.4- μm and 795-nm pulses at the sample, with FWHM bandwidths of 250 and 4.8 cm^{-1} , respectively.

The reflected beams from the sample are recollimated with a 10-cm FL lens. The 795-nm light is blocked by three dichroic mirrors (standard 800-nm-high reflectors); the SFG is polarization analyzed and then focused by a 10-cm FL lens into a 0.75-m spectrograph with 1200-groove/mm. The SF light is dispersed across a liquid-nitrogen-cooled, backthinned, scientific-grade CCD detector.⁹ The CCD array is 330 (V) \times 1100 (H, dispersing direction) pixels with a pixel size of 24 μm . Because it is focused through the entrance slit, the SFG typically covers only a few pixels in the vertical direction; these pixels are binned during data collection. The dispersion of the spectrograph at the SF (nominally 645 nm) is 0.023 nm (0.56 cm^{-1}) per bin; the inherent resolution of the spectrograph array is two bins.

Shown in Fig. 2 are BB SFG spectra for self-assembled monolayers (SAM's) of [trace (a)] fully deuterated octadecanethiol (d-ODT) and [trace (b)] fully hydrogenated octadecanethiol (ODT) on a Au film; we obtained the spectra by use of an IR pulse spanning the C—H stretch vibrational resonances. The spectra were acquired with *p*-polarized visible, IR, and SF beams. The acquisition time for each spectrum was 60 s. Observed spectral widths of SFG vibrational resonances were the same when 795-nm bandwidths of 2.0 or 4.8 cm^{-1} were used; broadening was observed at bandwidths of $\geq 6\text{ cm}^{-1}$. Peak signals typically correspond to ~ 350 detected photons per second per 0.56-cm^{-1} bin. The high-frequency

“hash” in the ODT and d-ODT spectra is not random noise but a recurrent etalon-type fringe pattern with 10-pixel spacing. Since a fully deuterated SAM has no vibrational resonances in this spectral region, one may take the ratio of the SFG spectrum of ODT to the SFG spectrum of d-ODT to account for the IR spectrum. As shown in trace (c) of Fig. 2, this normalization removes most of the etalon interference. The SF resonances show a derivativelike line shape owing to the interference between the resonant SAM response and the nonresonant Au response.²

The alkane chains of perfectly ordered ODT SAM's on Au are in a *trans*-extended configuration. CH_2 modes of all-*trans* alkane chains are symmetry forbidden in SFG, so only the terminal methyl resonances should be observed. The three prominent features seen in the SFG spectra of the ODT monolayer are in agreement with spectra reported in the literature¹⁰ and can be assigned to the $\text{CH}_3 \nu_s$ at 2877 cm^{-1} , the $\text{CH}_3 \nu_{\text{asy}}$ at 2964 cm^{-1} , and a Fermi resonance between the $\text{CH}_3 \nu_s$ and a CH_3 bend overtone at 2937 cm^{-1} . Methylene resonances are present in curve (c) of Fig. 2 as a small peak at 2850 cm^{-1} , assigned to the $\text{CH}_2 \nu_s$, and a broad band in the region from 2890 to 2930 cm^{-1} , attributable to either the $\text{CH}_2 \nu_{\text{asy}}$ or a Fermi resonance between the $\text{CH}_2 \nu_s$ and CH_2 bend overtones. The observation of methylene resonances indicates some disorder in this SAM from the all-*trans* configuration. The ability to detect and resolve the weak methylene resonances demonstrates the excellent signal-to-noise ratio and spectral resolution of our approach.

The BB SFG spectra are of remarkably good quality given the rapid acquisition time. Spectra of

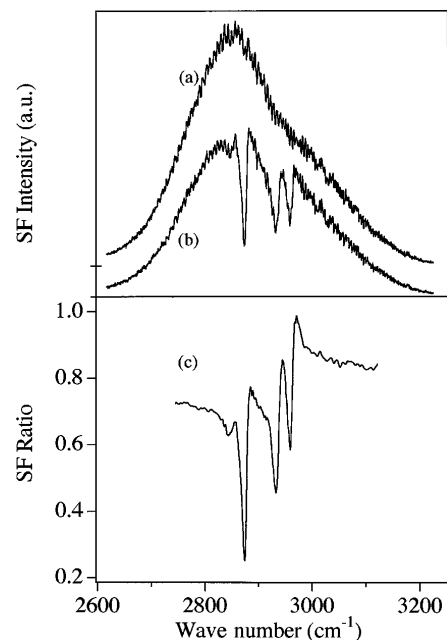


Fig. 2. SFG spectrum of a Au film covered with SAM's of (a) d-ODT and (b) ODT and (c) the ratio (b)/(a). The spectra were recorded in 60 s with *p*-polarized IR and visible incident beams and *p*-polarized detection of the SF. The visible bandwidth was 4.8 cm^{-1} . Traces (a) and (b) are offset vertically; a line indicating the zero signal is shown for each.

comparable quality were obtained in the C–D stretch region (2200–2000 cm^{-1}) for deuterated SAM's. Note that no pulse-to-pulse normalization of the spectra was done. As the entire spectrum is recorded on each laser shot, the system is quite insensitive to amplitude fluctuations. Since no tuning of the IR or the visible pulses occurs during spectral acquisition, the problem of maintaining constant spatial overlap while scanning is obviated. We obtained BB SFG spectra over the tuning range of 3 to 8 μm . In an experiment somewhat similar to ours, van der Ham *et al.* used the self-dispersive nature of noncollinear SFG to record (on a CCD array) spectra of thiophenol on Ag in the wavelength range 9.9–10.8 μm , using moderate bandwidth (25 cm^{-1} FWHM) IR light from a free-electron laser.¹¹ The present ultrafast source with spectrograph-dispersed SFG produces spectra over a much wider bandwidth.

As the stripped 795-nm beam has nominally constant power per unit bandwidth over the central 40 cm^{-1} , we can increase the pulse energy, and hence the SFG signal, by opening the monochromator exit slit to obtain the best balance between signal intensity and spectral resolution. In principle, the SFG signal amplitude will increase until the visible bandwidth becomes comparable with the natural linewidth of the sample, after which both the apparent width of the SF resonance and the integrated signal will increase. In practice, the relationship between the bandwidth of the visible pulse and the resolution of the SFG spectrum is simple only when the visible bandwidth is narrow or nearly transform limited.

Two other ways of generating visible mixing pulses were successfully tried. In one, the beam that was stripped from the compressor was sent directly to the sample (no bandwidth-limiting monochromator). Although it was approximately 50 cm^{-1} broad, the stripped beam was stretched in time (chirped 1.8 cm^{-1}/ps). Only the frequencies of the visible spectrum at the sample during the IR pulse, or within the dephasing time T_2 (the vibrational resonance FWHM $\Delta\nu = (\pi T_2)^{-1}$; for $\Delta\nu = 10.6 \text{ cm}^{-1}$, $T_2 = 1.0 \text{ ps}$), contribute to the width of the SFG. Although SFG spectra with resolution and signal-to-noise ratio similar to those of the spectra in Fig. 2 were obtained with this approach, it has two disadvantages. More visible light strikes the sample than contributes to the SFG signal, and the excess can cause sample damage. Also, the absolute frequency of the SFG vibrational features can vary within the 50- cm^{-1} envelope of the visible pulse, depending on alignment (timing) with respect to the IR; it was always necessary to use an absolute IR frequency reference (absorption cell with HCl gas) with this approach. Alternatively, the residual 800-nm pulses from the OPA (250 cm^{-1} FWHM; 500 μJ is not converted to signal and idler) were used. Before they went to the sample, the 0.15-ps pulses were stretched with a double-grating delay line; we controlled the chirp by varying the distance between the two grating passes. As with the preceding setup, the chirp determined the effective 800-nm bandwidth. Again, spectra similar to Fig. 2 were obtained. In

addition to the two problems mentioned above, this approach has the disadvantage that the spectrum of the residual 800 nm is strongly coupled to the operation of the OPA and can be severely distorted by nonlinear processes in the BBO crystal.

In conclusion, the method presented here for broad-bandwidth sum-frequency generation and parallel multichannel detection offers very fast data acquisition with a high signal-to-noise-ratio. Since complete spectral information is obtained on every laser shot, the method should be particularly useful for time-resolved studies. One example of use of this method is in ultrafast pump–probe experiments of vibrational dynamics at surfaces, the time resolution of which would be determined by the IR pulse duration (which could presumably be compressed to less than the present 0.2 ps). Another use for this method is in the study of phase transitions of films induced by changes in surface pressure or temperature, in which it is useful to obtain complete spectra rapidly as P or T is being ramped through the transition region.

T. P. Petralli-Mallow is a National Institute of Standards and Technology/National Research Council postdoctoral fellow.

John C. Stephenson's e-mail address is john.stephenson@nist.gov.

References

1. J. H. Hunt, P. Guyot-Sionnest, and Y. R. Shen, *Chem. Phys. Lett.* **133**, 189 (1987); P. Guyot-Sionnest, J. H. Hunt, and Y. R. Shen, *Phys. Rev. Lett.* **59**, 1597 (1988).
2. Y. R. Shen, *Nature (London)* **337**, 519 (1989); C. D. Bain, *J. Chem. Soc. Faraday Trans.* **91**, 1281 (1995); G. L. Richmond, *Anal. Chem.* **69**, A536 (1997).
3. Clark MXR Models IR-OPA and CPA 1000.
4. We identify certain commercial equipment, instruments, or materials in this Letter to specify adequately the experimental procedure. In no case does such identification imply recommendation or endorsement by the National Institute of Standards and Technology, nor does it imply that the materials or equipment identified are necessarily the best available for the purpose.
5. A Gaussian temporal shape was assumed to deconvolute all autocorrelation and cross-correlation measurements.
6. All reported stability measurements are 2σ based on 1000-shot averages.
7. F. Seifert, V. Petrov, and M. Woerner, *Opt. Lett.* **19**, 2009 (1994).
8. All reported beam dimensions are $1/e^2$ -intensity diameters.
9. Princeton Instruments Model LN/CCD-1100PB detector with an ST 138 controller.
10. A. L. Harris, C. E. D. Chidsey, N. J. Levinos, and D. N. Loiacono, *Chem. Phys. Lett.* **141**, 350 (1987); C. D. Bain, P. B. Davies, T. Hui Ong, R. N. Ward, and M. A. Brown, *Langmuir* **7**, 1563 (1991); M. A. Hines, J. A. Todd, and P. Guyot-Sionnest, *Langmuir* **11**, 493 (1995); M. S. Yeganeh, S. M. Dougal, R. S. Polizzotti, and P. Rabinowitz, *Phys. Rev. Lett.* **74**, 1811 (1995).
11. E. W. M. van der Ham, Q. H. F. Vreken, and E. R. Eliel, *Opt. Lett.* **21**, 1448 (1996).